bioRxiv preprint doi: https://doi.org/10.1101/2021.11.23.469641; this version posted April 13, 2022. The copyright holder for this preprint (which was not certified by peer review) is the author/funder, who has granted bioRxiv a license to display the preprint in perpetuity. It is made available under aCC-BY-NC-ND 4.0 International license.

Journal Title Here, 2019, pp. 1–13

doi: DOI HERE
Advance Access Publication Date: Day Month Year
Paper

PAPER

BatchDTA: Implicit batch alignment enhances deep learning-based drug-target affinity estimation

Hongyu Luo,[1,*] Yingfei Xiang,[1,*] Xiaomin Fang,[1,†] Wei Lin,[1] Fan Wang,[1,†] Hua Wu[2] and Haifeng Wang[2]

[1]Baidu Inc., 518000, Shenzhen, China and [2]Baidu Inc., 100000, Beijing, China
[*]Equal contributions.[†]Corresponding authors. fangxiaomin01@baidu.com, wang.fan@baidu.com
FOR PUBLISHER ONLY Received on Date Month Year; revised on Date Month Year; accepted on Date Month Year

Abstract

Candidate compounds with high binding affinities toward a target protein are likely to be developed as drugs. Deep neural networks (DNNs) have attracted increasing attention for drug-target affinity (DTA) estimation owning to their efficiency. However, the negative impact of batch effects caused by measure metrics, system technologies, and other assay information is seldom discussed when training a DNN model for DTA. Suffering from the data deviation caused by batch effects, the DNN models can only be trained on a small amount of "clean" data. Thus, it is challenging for them to provide precise and consistent estimations. We design a batch-sensitive training framework, namely BatchDTA, to train the DNN models. BatchDTA implicitly aligns multiple batches toward the same protein, alleviating the impact of the batch effects on the DNN models. Extensive experiments demonstrate that BatchDTA facilitates four mainstream DNN models to enhance the ability and robustness on multiple DTA datasets. The average concordance index (CI) of the DNN models achieves a relative improvement of 4.0%. BatchDTA can also be applied to the fused data collected from multiple sources to achieve further improvement.

Key words: Drug-target affinity, Deep neural network, Batch alignment, Batch effects

Introduction

Evaluation of drug-target affinity (DTA) (also known as receptor-ligand affinity) is one of the fundamental tasks for drug discovery. The drug-target binding affinity indicates the strength of binding interaction between the drug (ligand/compound) and target (receptor/protein). Laboratory experiments [27], e.g., in vivo and in vitro experiments, are usually involved in measuring the affinities between the protein to be studied and the candidate compounds. The compounds with the highest measured affinities are screened for further validation and could be future drugs. Since laboratory experiments are laborious, expensive, and time-consuming, some advanced studies employ efficient machine learning methods to estimate binding affinities, accelerating drug discovery. Machine learning methods [5, 26, 7, 6, 14], especially deep neural networks (DNNs) [31, 35, 32, 28, 34, 22, 30, 18, 29, 16], have gained increasing attention of many scholars, which utilize the affinity data collected from laboratory experiments to infer the affinities of other protein-compound interactions.

The Batch effects, as common effects in data from high-throughput laboratory experiments, have been widely discussed in many previous studies [24, 8]. This paper defines the batch effects as the systematic batch variation caused by differences in measure metrics, system technologies, laboratory conditions, reagents, and other assay information. Many published studies [1, 3] have shown that the systematic variation in experimentally collected data may lead to incorrect biological conclusions. Lots of techniques [23, 12, 38] have attempted to detect and adjust batch effects in laboratory experiments, but the negative impact of batch effects is still barely discussed in the field of DTA estimation, especially DTA estimation through DNN models.

The model parameters of the mainstream DNN models for DTA [31, 32, 22, 28, 18, 16] are usually optimized through the pointwise training framework, which minimizes the distance between the estimated affinity and the ground-truth affinity

© The Author 2019. Published by Oxford University Press. All rights reserved. For permissions, please e-mail: journals.permissions@oup.com

bioRxiv preprint doi: https://doi.org/10.1101/2021.11.23.469641; this version posted April 13, 2022. The copyright holder for this preprint (which was not certified by peer review) is the author/funder, who has granted bioRxiv a license to display the preprint in perpetuity. It is made available under aCC-BY-NC-ND 4.0 International license.

for each protein-compound interaction. Due to the lack of consideration of batch effects in model training, the DNN models trained by the pointwise framework is difficult to fully exploit the existing affinity data from multiple sources, measured by various techniques and systems, and could lead to the following issues:

First, the assays of affinity evaluation may adopt various metrics, e.g., dissociation constant (K_D), inhibition constant (K_I), half-maximal inhibitory concentration (IC_{50}), and half-maximal effective concentration (EC_{50}), to measure the binding affinities. The affinity values evaluated through different metrics are usually incomparable (refer to Appendix B). A DNN model trained by the pointwise framework is confused by the multifarious incomparable "affinities" from multiple assays/batches of the same protein-compound interaction, thus struggling to provide a consistent estimation. Previous academic works tend to train a DNN model on the data points measured by the same metric to get around the metric incomparability issue. Nevertheless, the data points with respect to a specific metric are insufficient to train a capable DNN model, usually with numerous parameters and thus requiring lots of training data points.

Second, even though only utilizing those data points of a specific metric to train a model, the trained model still suffers from variance caused by other assay information. For example, some metrics, e.g., IC_{50} and EC_{50}, are highly assay-specific [19], and the measured affinities under different assay settings are incomparable. The DNN model is confounded by the multifarious "affinities" from multiple assays of the same protein-compound interaction, thus struggling to provide consistent estimates.

Consequently, the batch effects caused by various metrics, assay settings, and other factors obstruct advanced DNN models from fully exploiting the collected data points or achieving more satisfactory precision. It is attractive to take advantage of fuse multi-source data points with various assay settings and align these data points to further enhance the DNN model's ability.

To facilitate the effectiveness of the DNN models for DTA, we attempted to alleviate the negative impact of batch effects through a batch-sensitive training framework, namely BatchDTA. BatchDTA learns the ranking orders of the comparable protein-compound interactions in the same batch. In this way, the interactions of a protein from multiple batches can be implicitly aligned by taking those interactions that simultaneously appeared in multiple batches as the reference for comparison. Extensive experiments are conducted to verify that through training with BatchDTA framework, multiple mainstream DNN models, including DeepDTA [31], GraphDTA [28], and MolTrans [16], can achieve higher concordance indexes (CIs) and lower deviation. We also visualize a case to demonstrate that BatchDTA can successfully learned the ranking orders of the compounds from different batches through the reference interaction. Furthermore, BatchDTA is applied to utilize fused data points measured by multiple metrics from multiple sources as the training data. The concordance indexes (CIs) [11] of the DNN models are promoted in most cases, exhibiting the potential practical value of BatchDTA.

Our main contributions can be summarized as follows:

1. We utilize a batch-sensitive training framework, called BatchDTA, to alleviate the harmful influence of the batch effects for DTA prediction.
2. BatchDTA aims to implicitly align multiple batches for the same target protein by learning the ranking orders of the interactions within a batch.
3. Extensive experiments demonstrate that BatchDTA can facilitate the precision and robustness of multiple mainstream DNN models in multiple situations.

Materials and Methods

Problem Formulation

Advanced proposed DNN models for DTA utilize the pointwise training framework, which regards DTA estimation as a classification or regression problem. Since the goal of the DTA estimation task is locating those compounds with higher affinities toward a target protein, we regard the task of DTA estimation as a ranking problem instead. More concretely, a ranking task of DTA is defined as a batch (or an assay) with batch $b = (p, \mathcal{C})$, containing a protein p and a set of the candidate compounds $\mathcal{C}$. The set of candidate compounds is defined as $\mathcal{C} = \{c_i\}|_{i=1}^{n_c}$, where $n_\mathcal{C}$ represents the number of candidate compounds in the corresponding batch. We expect to screen out the most promising compounds in $\mathcal{C}$ as the potential drugs for target protein p for batch b. Usually, hundred to tens of thousands of batches can be collected from a data source, $\mathcal{S} = \{(b_i, \mathbf{y}_i)\}|_{i=1}^{n_s}$, where n_s represents the number of batches in data source $\mathcal{S}$. The set of the corresponding labels, i.e., collected affinities, of the candidate compounds $\mathcal{C}$ in batch b is denoted by $\mathbf{y} = \{y_i\}|_{i=1}^{n_c}$. Additionally, we attempt to simultaneously exploit the data from various data sources $\{\mathcal{S}_i\}|_{i=1}^{n_\mathcal{S}}$ to train the DNN models for DTA to test the prospect of data fusion, where $n_\mathcal{S}$ denotes the number of data sources.

Implicit Batch Alignment

We attempt to align a target protein's corresponding protein-compound interactions from multiple batches. Those interactions are implicitly aligned through the reference interactions that simultaneously appear in multiple batches. The demonstration of implicit batch alignment is shown in Fig. 1, and the details will be introduced in the following.

We first define the ranking order of two compounds concerning a batch. Since two interactions from different batches may target different proteins or their corresponding affinities may be evaluated under different assay settings, the ranking orders of most compound pairs are valueless. Thus, we concentrate on learning the ranking order of two candidate compounds c_i and c_j for a given batch $b = (p, \mathcal{C})$. To formalize, we introduce a new operator $>_b$ for comparison of two compounds. Formula $c_i >_b c_j$ indicates the affinity of compound c_i measured by a assay is significantly larger than that of compound c_j for the same batch b. Since affinities measured by the laboratory assays are usually noisy, a hyper-parameter, i.e., deviation ϵ, is introduced to determine whether the two measured affinities differ significantly. More concretely, formula $c_i >_b c_j$ indicates that $y_i > y_j + \epsilon$, where y_i and y_j denotes the assay-measured affinities of compound c_i and compound c_j in the compound set $\mathcal{C}$ of the batch $b = (p, \mathcal{C})$. Then, for a batch $b = (p, \mathcal{C})$, we can theoretically generate $\mathcal{O}(n_\mathcal{C}^2)$ training pairs of compounds: $\{(c_i, c_j), s.t., c_i >_b c_j\}_{i,j=1}^{n_c}$. We define the training dataset as $\mathbf{D} = \{(p, c_i, c_j), s.t., (b, \mathbf{y}) \in \mathcal{S}_k, b = (p, \mathcal{C}), c_i >_b c_j\}|_{k=1}^{n_\mathcal{S}}$. Pair (c_i, c_j) is called a training pair as demonstrated on the left of Fig. 1, and triple (p, c_i, c_j) is called a training sample.

Draft

bioRxiv preprint doi: https://doi.org/10.1101/2021.11.23.469641; this version posted April 13, 2022. The copyright holder for this preprint (which was not certified by peer review) is the author/funder, who has granted bioRxiv a license to display the preprint in perpetuity. It is made available under aCC-BY-NC-ND 4.0 International license.

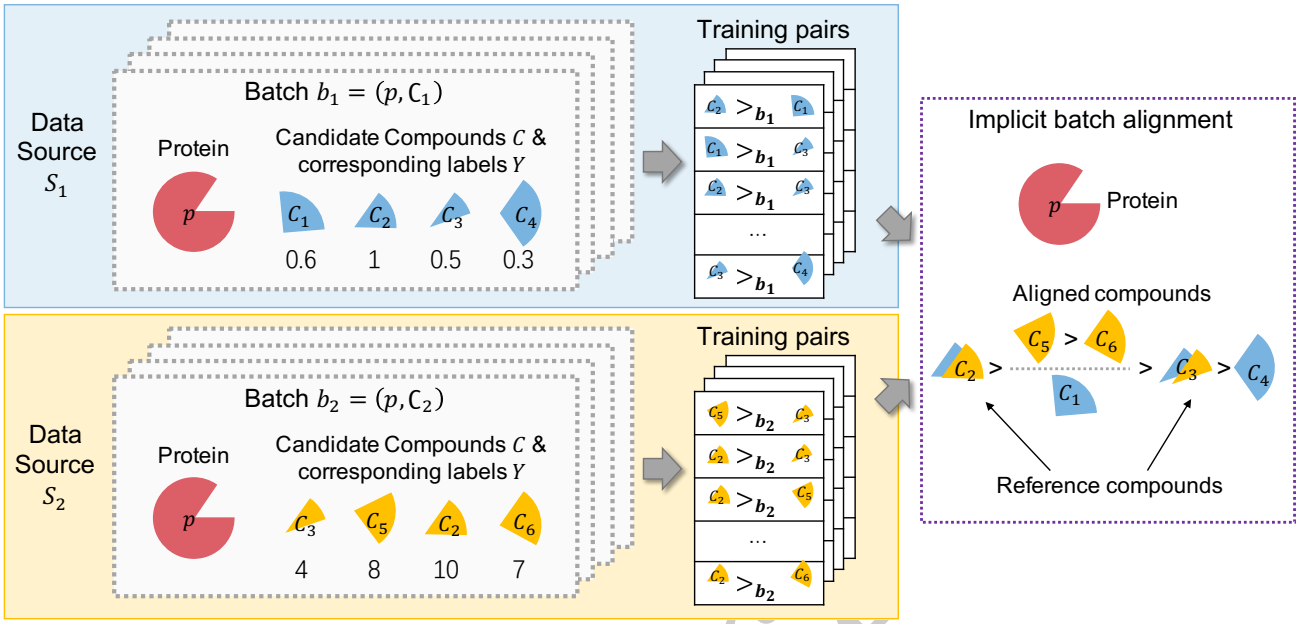

Fig. 1. Implicit batch alignment. Compound pairs for training are generated from each batch. The compounds in multiple batches for the same protein are implicitly aligned through the compounds in both batches. (Notched circles represent proteins and sectors of various colors represent compounds)

Then, we introduce reference compounds to align the interactions from different batches. A reference compound is defined as a compound that appears in multiple batches toward the same protein. Given a protein p, there might be multiple batches studying that protein. We assume both batch $b_1 = (p, \mathcal{C}_1)$ and batch $b_2 = (p, \mathcal{C}_2)$ study protein p. A reference compound c^{ref} should satisfy that $c^{ref} \in \mathcal{C}_1 \wedge c^{ref} \in \mathcal{C}_2$. For batch $b_1 = (p, \mathcal{C}_1)$, we denote the compounds in $\mathcal{C}_1$ with the corresponding ground-truth affinities smaller than that of the reference compound c^{ref} as $\mathcal{C}_1^{worse}$. For batch $b_2 = (p, \mathcal{C}_2)$, the compounds in $\mathcal{C}_2$ with the corresponding ground-truth affinities larger than that of the reference compound c^{ref} as $\mathcal{C}_2^{better}$. It is likely the affinity of compound $c_2 \in \mathcal{C}_2^{better}$ is larger than that of compound $c_1 \in \mathcal{C}_1^{worse}$. In this way, the compounds from different batches can be implicitly aligned. A toy case is exhibited in Fig. 1. Both the batch $b_1 = (p, \mathcal{C}_1)$ in data source S_1 and the batch $b_2 = (p, \mathcal{C}_2)$ in data source S_2 study the protein p, where $\mathcal{C}_1 = \{c_1, c_2, c_3, c_4\}$ and $\mathcal{C}_2 = \{c_3, c_5, c_2, c_6\}$. Due to the batch effects, the affinity values collected from various sources are incomparable (e.g., from 0.3 to 1.0 in batch b_1 and from 4 to 10 in batch b_2). Training pairs (compound pairs) are extracted from each batch based on the ranking order of the compounds. The training pairs from different batches with respect to protein p are collected. As compound c_3 appear in $\mathcal{C}_1$ and $\mathcal{C}_2$, compound c_3 is taken as a reference compound. Though the reference compound c_3, compound c_4 from batch b_1, compounds c_5, and c_6 from batch b_2 become comparable.

Since compounds from different batches are comparable through implicit batch alignment, we can effortlessly fuse the data points from multiple sources to train a more capable model for DTA.

Learning the Ranking Orders

Many studies utilized deep neural networks (DNNs) to predict the affinity between proteins and compounds, including DeepDTA [31], GraphDTA [28], and MolTrans [16]. We train these DNN models by learning the ranking orders of the training pairs.

A typical DNN model for DTA prediction consists of three components: Protein Encoder, Compound Encoder, and Interaction Estimator, as shown on the left of Fig. 2.

- **Protein Encoder.** The primary structure of a protein is described by an amino acid sequence. A Protein Encoder applies various kinds of sequence-based neural networks, e.g., Convolutional Neural Networks (CNNs) [21, 20] and Transformers [37], to produce the representation vectors of the proteins. We formalize the Protein Encoder as a function $f_{protein}(p; \Theta_P)$, taking a protein p as input, where Θ_p represents the corresponding model parameters. The representation vector of a protein p is defined as $h_p = f_{protein}(p; \Theta_P)$.
- **Compound Encoder.** A Compound Encoder typically generates the compounds' representation vectors through molecular fingerprints (e.g., ECFP [33] and MACCS [10]), sequence-based representation methods (e.g., LSTMs [15] and Transformers), or graph-based representation methods (e.g., GNNs). We describe the Compound Encoder as a function $f_{compound}(c; \Theta_C)$, taking a compound c as input, where Θ_C represents the model parameters needed to be optimized. Then, the representation vector of a compound c can be written as $h_c = f_{compound}(c; \Theta_C)$.
- **Interaction Estimator.** The Interaction Estimator estimates the interaction score between a protein p and a compound c in accordance to a function $f_{interation}(h_p, h_c; \Theta_I)$, where Θ_I denotes the function's learnable parameters. Function $f_{interation}(h_p, h_c; \Theta_I)$ takes the representation vectors h_c and h_p as inputs and outputs an estimated affinity score.

The parameters of whole model $f(p, c; \Theta)$ can be formulated as Eq. 1, combining $f_{protein}(p; \Theta_P)$, $f_{compound}(c; \Theta_C)$, and

Draft

bioRxiv preprint doi: https://doi.org/10.1101/2021.11.23.469641; this version posted April 13, 2022. The copyright holder for this preprint (which was not certified by peer review) is the author/funder, who has granted bioRxiv a license to display the preprint in perpetuity. It is made available under aCC-BY-NC-ND 4.0 International license.

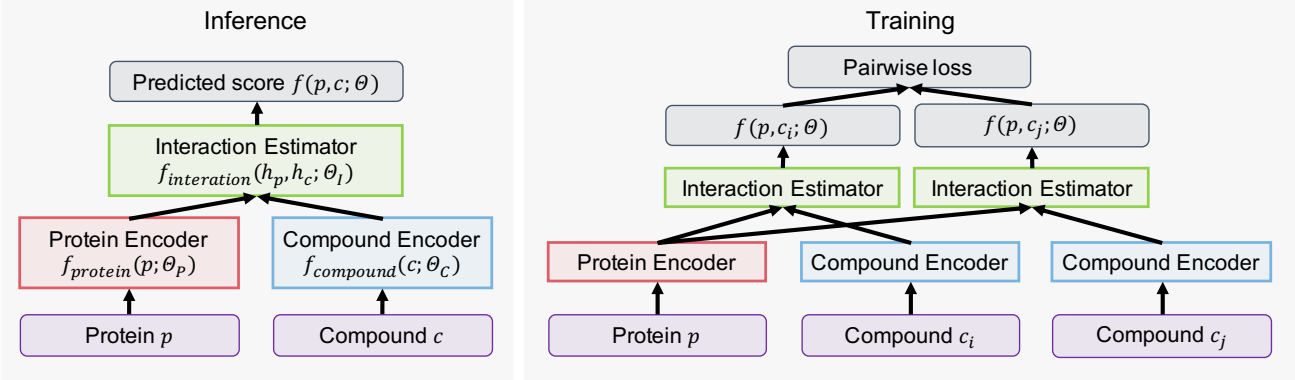

Fig. 2. Inference of a typical DNN model $f(p, c; \Theta)$ for DTA and the training framework that trains the DNN model $f(p, c; \Theta)$ through learning the ranking orders of the candidate compounds.

$f_{interaction}(h_p, h_c; \Theta_I)$:

$$f(p, c; \Theta) = f_{interaction}(f_{protein}(p; \Theta_P), f_{compound}(c; \Theta_C); \Theta_I). \tag{1}$$

where $\Theta = \{\Theta_C, \Theta_P, \Theta_I\}$ are the model parameters need to be optimized. The candidate compounds are ranked in accordance with the affinities estimated by the DNN model $f(p, c; \Theta)$, and the compounds with the highest estimated affinities are selected as promising drugs for further validation.

Advanced studies optimize the model parameters Θ to minimize the absolute error between the assay-measured affinity and the model-estimated affinity of a protein-compound pair. In contrast to the previously applied training framework (pointwise training), we adopt a pairwise training framework to optimize the ranking orders of the candidate compounds of a given batch, as shown on the right of Fig. 2. More concretely, the pairwise training framework takes the sample $(p, c_i, c_j) \in \mathbf{D}$ as input to learn the order of compounds c_i and c_j with respect to protein p. Following the classical pairwise ranking method RankNet [4], we regard the pairwise order learning problem as a binary classification task, where the cross-entropy is used as the loss function for the sample $(p, c_i, c_j) \in \mathbf{D}$:

$$\begin{aligned} L(p, c_i, c_j; \Theta) =& - \hat{P}_{p,c_i,c_j} log P_{p,c_i,c_j} \\ & - (1 - \hat{P}_{p,c_i,c_j}) log(1 - P_{p,c_i,c_j}), \\ \hat{P}_{p,c_i,c_j} =& \delta(y_i, y_j), \\ P_{p,c_i,c_j} =& \frac{exp(o_{p,c_i,c_j})}{1 + exp(o_{p,c_i,c_j})}, \\ o_{p,c_i,c_j} =& f(p, c_i; \Theta) - f(p, c_j; \Theta). \end{aligned} \tag{2}$$

$\hat{P}_{p,c_i,c_j}$ indicates whether the ground-truth affinity score of compound c_i, i.e., y_{p,c_i} is larger than that of compound c_j, i.e., y_{p,c_j}. $\delta(x, y)$ is an indicator function that $\delta(x, y) = 1$ if $x > y$, and $\delta(x, y) = 0$ if $x \leq y$. Besides, P_{p,c_i,c_j} represents the model-estimated probability whether the affinity of compound c_i is larger than that of compound c_j. P_{p,c_i,c_j} applies Sigmoid function [13] on o_{p,c_i,c_j}, i.e., the difference between the estimated affinities $f(p, c_i; \Theta)$ and $f(p, c_j; \Theta)$. The cross-entropy between the ground-truth probability $\hat{P}_{p,c_i,c_j}$ and the estimated probability P_{p,c_i,c_j} is minimized to learn the model parameters of the DNN model $f(p, c; \Theta)$. As an affinity pair $(p, c_i, c_j) \in \mathbf{D}$ satisfies $c_i >_b c_j$ and $y_i > y_j$, $\hat{P}_{p,c_i,c_j} = 1$, the loss function for a sample (p, c_i, c_j) in Eq. 2 can be simplified as

$$\begin{aligned} L(p, c_i, c_j; \Theta) &= -log \frac{exp(o_{p,c_i,c_j})}{1 + exp(o_{p,c_i,c_j})}, \\ o_{p,c_i,c_j} &= f(p, c_i; \Theta) - f(p, c_j; \Theta). \end{aligned} \tag{3}$$

Then, the overall loss function of dataset $\mathbf{D}$ is defined as

$$L(\mathbf{D}; \Theta) = \sum_{(p,c_i,c_j) \in \mathbf{D}} L(p, c_i, c_j; \Theta). \tag{4}$$

We minimize the loss function $L(\mathbf{D}; \Theta)$ to optimize the model parameters of $f(p, c; \Theta)$.

As we mentioned above, we can theoretically produce $\mathcal{O}(n_C^2)$ samples for a batch $b = (p, \mathcal{C})$. In order to balance the effects of different batches for training, we randomly sample n_{sample} samples for each compound within a batch b at each iteration, where N is the sampling times. In this way, for each batch, only $O(n_{sample} \cdot n_C)$ samples are exploited for training at each iteration.

Results

We use the pointwise framework and BatchDTA to train multiple advanced DNN models, respectively, to observe the effect of BatchDTA.

Datasets

The DNN models are trained on three DTA datasets, including BindingDB [25], Davis [9], and KIBA [36]. The BindingDB dataset collected affinities with various metrics (K_D, K_I, IC_{50}, and EC_{50}) and other assay information from multiple data sources. The affinities in the Davis dataset are measured by K_D, while those in the KIBA dataset are indicated by the KIBA score that integrates multiple bioactivity types, i.e., K_D, K_I, and IC_{50}. These datasets are processed to filter out the invalid protein-compound interactions (refer to Appendix. A) for data processing).

Previous DTA studies [28, 18, 32] randomly split the protein-compound interactions of a dataset into a training set and a test set. However, random splitting over-simplifies the task of DTA. Due to multiple batches, a target protein in the test set could have already been observed in the training set, resulting in information leakage and model overfitting. Therefore, we split the datasets on the basis of batches and ensure that the proteins

Draft

bioRxiv preprint doi: https://doi.org/10.1101/2021.11.23.469641; this version posted April 13, 2022. The copyright holder for this preprint (which was not certified by peer review) is the author/funder, who has granted bioRxiv a license to display the preprint in perpetuity. It is made available under aCC-BY-NC-ND 4.0 International license.

observed in the training set will not appear in the test set, which is more in line with the real-world applications. For each dataset, we strive to identify the batches based on the available assay information recorded in the corresponding dataset. Since the batch IDs are not recorded in the datasets, we can not completely guarantee the accuracy of batch identification (refer to Appendix. A for batch identification of each dataset). The statistics of the datasets are shown in Tab. 2.

DNN Models for DTA

We compare two training frameworks, *Pointwise* and *BatchDTA*, by applying them to three previously proposed DNN models for DTA:

- **DeepDTA** [31] employs three-layers Convolutional Neural Networks (CNNs) as Protein Encoder and Compound Encoder to encode the protein sequences and the compound SMILES strings, respectively. Then, for the Interaction Estimator, the encoded protein and compound are concatenated to predict the affinity score.
- **GraphDTA** [28] regards each compound as a graph and attempts several GNNs, such as GIN, GAT, GCN, and GAT-GCN, as the Compound Encoders to represent the compounds. In the meantime, GraphDTA regards each protein as a sequence and adopts CNNs as the Protein Encoder to encode the proteins. The Interaction Estimator is the same as DeepDTA's. In this paper, we implement two versions of GraphDTA, denoted by GraphDTA(GCN) and GraphDTA(GATGCN), respectively.
- **MolTrans** [16] decomposes the compounds' SMILES strings and the proteins' acid amino sequences into high-frequency sub-sequences. Then, it applies Transformers as the Compound Encoder and Protein Encoder to obtain the augmented representation with the chemical semantics. MolTrans uses the outer-product operator and CNN blocks as Interaction Estimator to capture the high-order interaction between the compounds and proteins.

For all the DNN models, we use the hyper-parameters suggested by the corresponding papers.

Training and Evaluation Settings

We follow the settings of the previous works to implement *Pointwise* framework, where the mean squared error (MSE) between the models' predicted values and the ground-truth affinities are taken as the loss function to optimize the model parameters. For the *BatchDTA* framework, we apply grid search to search the hyper-parameters, including sample times, learning rate, and batch size. The details of hyper-parameter settings are described in Appendix C.1.

Concordance Index (CI) [11] is used to evaluate the performance of *Pointwise* and *BatchDTA* training frameworks in terms of batches. The CI for a given batch $b = (p, \mathcal{C})$ is defined as:

$$CI(b) = \frac{1}{z} \sum_{c_i, c_j \in \mathcal{C}} I(y_i - y_j) \cdot I(f(p, c_i; \Theta) - f(p, c_j; \Theta)), \quad (5)$$

where $z = \sum_{c_i, c_j \in \mathcal{C}} I(y_i - y_j)$, and $I(.)$ is an indicator function. $I(x) = 1$ if $x > \epsilon^*$, and $I(x) = 0$ otherwise. ϵ^* is used to identify the compound pairs with large gap of their corresponding affinities. ϵ^* set to be 0 by default unless otherwise specified.

Then, we define the overall CI for all the test batches $\mathcal{B} = \{b_i\}|_{i=1}^{n_\mathcal{B}}$ by summarizing $CI(b)$, where $n_\mathcal{B}$ is the number of test batches. The overall CI is formalized as

$$CI = \frac{1}{\sum_{b \in \mathcal{B}} w(b)} \sum_{b \in \mathcal{B}} w(b) CI(b), \quad (6)$$

where $w(b) = n_\mathcal{C}$ for task $b = (p, \mathcal{C})$ is introduced to balance the impact of different batches.

Overall Performance

To verify that implicit batch alignment can alleviate the negative impact of batch effects, we trained multiple previously proposed DNN models for DTA through the *Pointwise* and *BatchDTA* training frameworks, respectively. We expect a DNN model trained by *BatchDTA* framework can achieve further improvement compared with that trained by *Pointwise* framework.

Database BindingDB records the affinities of millions of protein-compound interactions measured by various metrics. Most data points in BindingDB are measured by metrics inhibition constant (K_I) and half-maximal inhibitory concentration (IC_{50}). Two hundred thousand protein-compound interactions from ten thousand batches are measured by K_I, while six hundred thousand interactions from twenty thousand batches are measured by IC_{50} (refer to Table 2 for statistics of the datasets). Since the assay information, such as temperature, pH degree, and competitive substrate, affect the values of K_I and IC_{50}, the data points measured by K_I and IC_{50} are suitable for verifying whether *BatchDTA* can effectively mitigate the impact of batch effects. The dataset of each metric is divided into the training set, validation set, and test set by 8:1:1. A model is trained on the training set with the best epoch selected by the validation set. For each experimental setting, we trained each model five times and evaluated the CIs on all the compound pairs ($\epsilon^* = 0$) as well as the confident compound pairs ($\epsilon^* = 0.6$) in the test set. Confident compound pairs are introduced to diminish the impact of the experimental variance for the evaluation. We eliminated the compound pairs with small affinity gaps from all the compound pairs, and the remaining pairs are called confident compound pairs (refer to Appendix C.2) for details of confident compound pairs generation).

Fig. 3 shows the CIs of four DNN models trained by *Pointwise* framework and *BatchDTA* framework. We can draw the following conclusions:

- Since *BatchDTA* is a batch-sensitive training framework, it can make more rational use of the collected data points than the *Pointwise* framework, which could further enhance the ability and robustness of a DNN model for DTA. *BatchDTA* framework significantly outperforms *Pointwise* framework under 14/16 settings. Besides, in most cases, the standard deviation of CIs of the model trained by the *Pointwise* framework is greater than that by the *BatchDTA* framework. We suspect that the conflicting data between batches cause the larger variance of the model trained by the *Pointwise* framework.
- For each DNN model, the relative improvement of *BatchDTA* compared with *Pointwise* is higher when evaluating on the confident compound pairs than on all the compound pairs. Since the gaps between the measured affinities of some compounds in a batch are not significant, excluding those incomparable compound pairs in the evaluation can highlight the advantages of *BatchDTA*. For example, for K_I, *BatchDTA* achieves an average relative

Draft

bioRxiv preprint doi: https://doi.org/10.1101/2021.11.23.469641; this version posted April 13, 2022. The copyright holder for this preprint (which was not certified by peer review) is the author/funder, who has granted bioRxiv a license to display the preprint in perpetuity. It is made available under aCC-BY-NC-ND 4.0 International license.

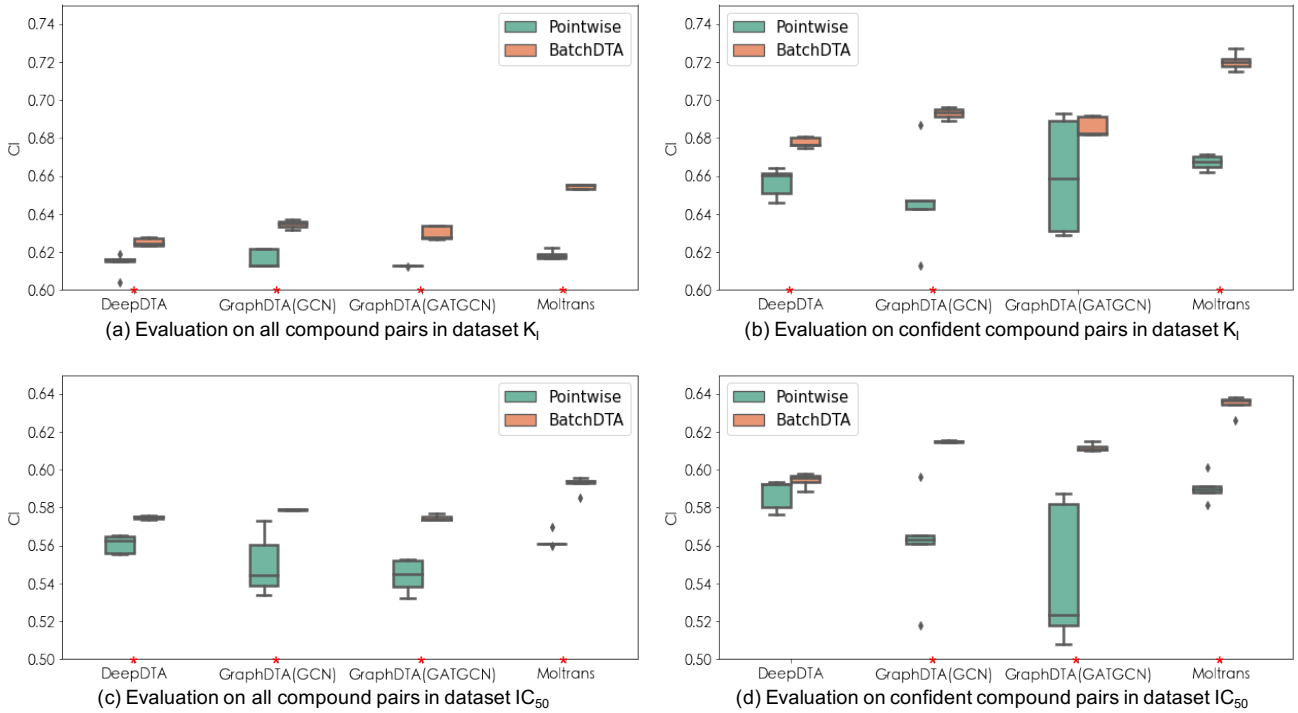

Fig. 3. Comparing the CIs of the DNN models trained by *Pointwise* framework and *BatchDTA* framework on database BindingDB under different settings. (A red star stands for statistical significance with P-value less than 0.05 for a two-tailed test.)

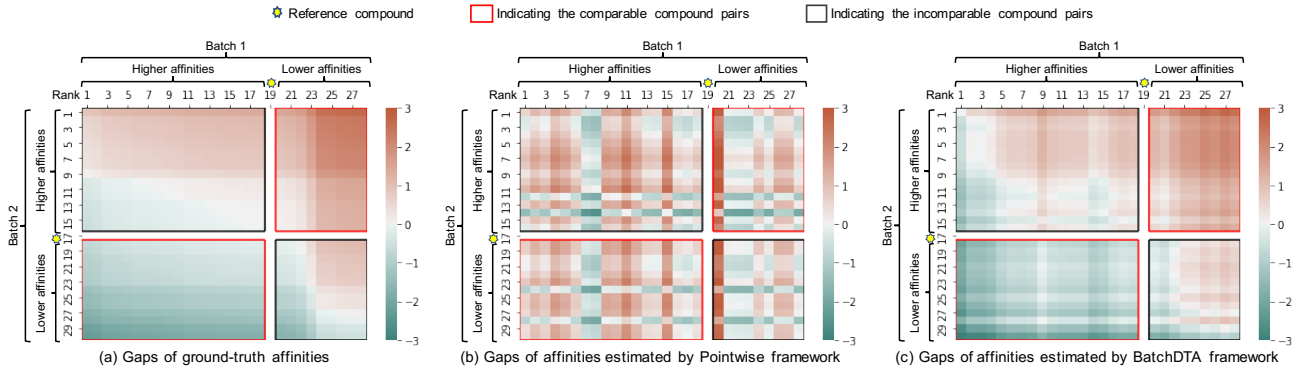

Fig. 4. Case study analyzing whether *Pointwise* framework and *BatchDTA* framework can learn the ranking orders of the compound from two batches for the same protein.

improvement of 3.2% on all the compound pairs, while 5.5% on the confident compound pairs. For IC_{50}, the average relative improvement is 4.7% for all the compound pairs and 7.8% for confident compound pairs.

- Compared with K_I, IC_{50} is also affected by the concentration of enzyme and substrate, and thus the systematic variance of the assays measured by IC_{50} is larger than that measured by K_I. The larger variance makes a DNN model more difficult to provide accurate estimations on the IC_{50} dataset, but we can observe that all the DNN models trained by *BatchDTA* can still achieve further improvement.

Case Study

We further explore whether *BatchDTA* can successfully align and learn the ranking orders of the compounds from multiple batches by case study. We selected a case of two batches toward the same protein from the training set of IC_{50} with a reference compound appearing in both batches. The reference compound is expected to implicitly align the compounds from two batches. In Fig. 4, we visualize three matrices with each element representing the affinity gap between a compound in Batch 1 and a compound in Batch 2. The affinity gaps are normalized, and the darker the color in the matrices, the greater the affinity gap. More concretely, we sorted compounds in Batch 1 and Batch 2 according to the ground-truth affinities, respectively. For each matrix, each column stands for a compound from Batch 1, each row stands for a compound for Batch 2, and each element stands for a compound pair

bioRxiv preprint doi: https://doi.org/10.1101/2021.11.23.469641; this version posted April 13, 2022. The copyright holder for this preprint (which was not certified by peer review) is the author/funder, who has granted bioRxiv a license to display the preprint in perpetuity. It is made available under aCC-BY-NC-ND 4.0 International license.

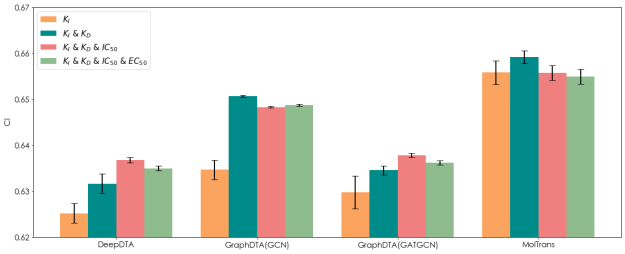

Fig. 5. Exploring the performance of the DNN models trained on the fused data points measured by multiple metrics, i.e., K_I, K_D, IC_{50}, and EC_{50} by *BatchDTA* framework.

with its color indicating the affinity gap. The three matrices describe the gaps between the ground-truth affinities collected in the dataset, the gaps between the predicted affinities of the MolTrans model trained by the *Pointwise* framework, the gaps between the predicted affinities of the MolTrans model trained by *BatchDTA* framework, respectively.

In general, the color pattern of the gaps of affinities estimated by *BatchDTA* framework (Fig. 4(c)) is similar to that of the gaps of ground-truth affinities (Fig. 4(a)). The colors in both the ground-truth matrix and *BatchDTA* matrix transition smoothly, with dark red at the upper right, dark green at the lower left, and white at the diagonal. The consistent color patterns reveal that *BatchDTA* can well learn the ranking order of a compound pair with one compound in Batch 1 and the other in Batch 2. In contrast, the color pattern of *Pointwise* is chaotic, which is distinct from that of the ground-truth. More specifically, the grids (compound pairs) in a matrix can be divided into two portions: the comparable compound pairs indicated by the red boxes (lower left and upper right) and the incomparable compound pairs indicated by the black boxes (lower right and upper left). For example, the compounds with higher affinities than the reference compound in Batch 1 (the first 18 columns) should rank ahead of those with lower affinities than the reference compound in Batch 2 (the last 13 rows). Thus, the corresponding compound pairs indicated by the red box at the lower left are regarded as comparable compound pairs. The model trained by *BatchDTA* can infer the compounds' ranking order with a high certainty (indicated by darker color) for most of the comparable compound pairs. For the incomparable compound pairs, although the model trained by *BatchDTA* can not determine some compounds' ranking order, e.g., the ranking order of the first compound in Batch 1 and the first compound in Batch 2, the overall ranking predictions are consistent with those of the ground-truth.

Fusing Data

The *BatchDTA* framework can also be applied to the fused data points collected from multiple sources. It is attractive to take advantage of fused data points to train the DNN models for DTA. Therefore, we explore the practicality of *BatchDTA* in two data fusion scenarios: fusing data measured with multiple metrics and fusing data from multiple open-source datasets.

Fusing Data Points Measured by Multiple Metrics

We utilized the database BindingDB and trained the DNN models on the fusing data measured with multiple metrics. Each DNN model is trained on four datasets, i.e., K_I, K_I&K_D, K_I&K_D&IC_{50}, and K_I&K_D&IC_{50}&EC_{50}, respectively by *BatchDTA* framework, where operator & denotes fusing the data points measured by different metrics. The trained DNN models are evaluated on the test set of K_I. We consider the correlations between the metrics (refer to Appendix B) when designing the experiments. Since the metrics with higher correlations to K_I are more likely to provide advantages to the DNN models that only trained on the data points of K_I, we first integrated the data points of K_D into the training set, then those of IC_{50}, and finally those of EC_{50}. Each experiment is run five times, and the performance of the DNN models trained on the fused data points measured by multiple metrics is shown in Fig. 5. We can observe the following phenomena: (1) By adding the data points of K_D to the training set, all the DNN models gain significant performance improvement (average relative improvement of 1.21%). Since K_I and K_D have a strong correlation (Pearson r=0.83), the data points of K_D potentially augment valuable information. (2) Due to the higher systematic deviations of the data measured by IC_{50} and EC_{50}, the correlation between K_I and IC_{50} as well as the correlation between K_I and EC_{50} are relatively low (Pearson r=0.74 and 0.64, respectively). Thus, fusing the data points of IC_{50} and EC_{50} can not further significantly raise the accuracy of the DNN models. These phenomena enlighten us that integrating high correlation data into the training set could improve the effectiveness of existing DNN models on DTA.

Fusing Data Points from Multiple Datasets

Datasets Davis and KIBA are utilized to explore the potential of *BatchDTA* when training the DNN models on the fused data points collected from multiple datasets. Since these two datasets contain only hundreds of batches (refer to Table 2 in Appendix), we perform 5-fold cross-validation [2] to reduce the evaluation deviation. When evaluating the DNN models on the Davis dataset, we compare three training methods: *Pointwise (Davis)* and *BatchDTA (Davis)* that only utilize the Davis dataset for training, as well as *BatchDTA (Davis + KIBA)* that utilize both the datasets Davis and KIBA for training. The setting is similar when evaluating the DNN models on the KIBA dataset. Fig. 6 exhibits the comparison of the DNN models trained on the fused data points collected from multiple datasets. As we expected, the CIs of the DNN models trained on only one dataset by *BatchDTA* framework surpass those by *Pointwise* framework, which is consistent with the evaluation results of Fig. 3 on database BindingDB. Furthermore, by combining the datasets Davis and KIBA for training, the DNN models trained by *BatchDTA* achieve better performance in general. The better results of the fused datasets illustrate that as a DNN model usually requires lots of training data, the additional data points for training are likely to benefit the ability of the DNN models for DTA.

Discussion

Many published literature have discussed the impact of batch effects, but little work has been done to explore the batch effects on the DNN models for DTA. Table 1 reports the data analysis of the database BindingDB. We attempt to analyze the impact scope of batch effects for DTA through the dimensions of proteins and batches (the first two rows in Table 1) and investigate which group of the impacted data points (the last row in Table 1) can be effectively taken advantage of by BatchDTA to achieve better results. From the table, we can observe: (1) About 40% of proteins simultaneously appear in multiple batches, and the collected affinities of corresponding

Draft

bioRxiv preprint doi: https://doi.org/10.1101/2021.11.23.469641; this version posted April 13, 2022. The copyright holder for this preprint (which was not certified by peer review) is the author/funder, who has granted bioRxiv a license to display the preprint in perpetuity. It is made available under aCC-BY-NC-ND 4.0 International license.

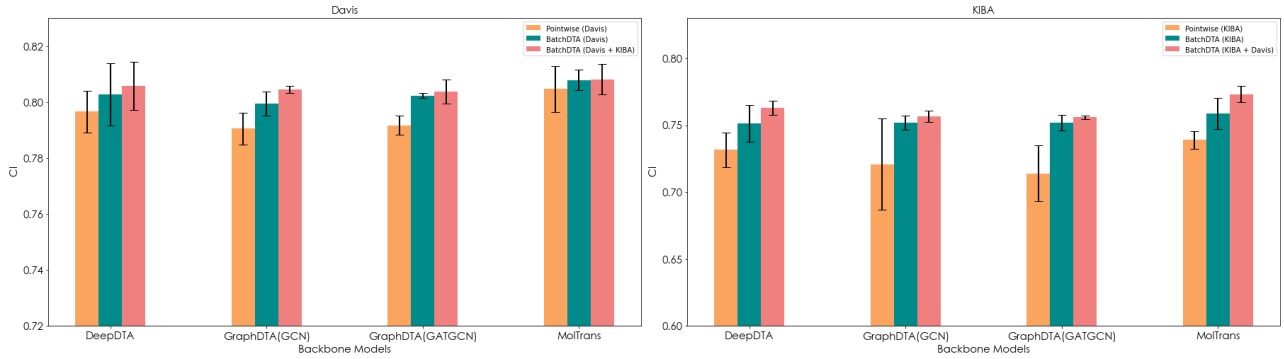

Fig. 6. Exploring the performance of the DNN models trained on the fused data points collected from multiple datasets, i.e., Davis and KIBA, by *BatchDTA* framework.

Table 1. Data analysis of dataset BindingDB.

	K_D	K_I	IC_{50}	EC_{50}	All
Proteins appearing in multiple batches	40.0%	42.2%	40.5%	36.1%	44.0%
Batches with interactions appearing in another batch	43.3%	55.7%	48.5%	48.6%	57.9%
Inconsistent ranking orders	12.4%	8.1%	7.1%	14.6%	13.9%

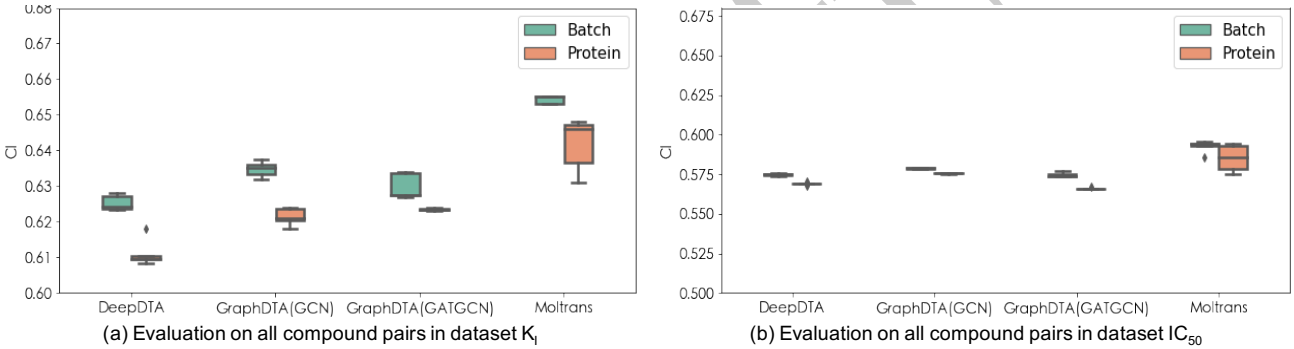

Fig. 7. Impact of the quality of batch identification methods.

data points could be inconsistent. A batch-sensitive training framework is demanded to alleviate the negative impact of those inconsistent data points. (2) There are 43.3% to 55.7% of batches with interactions appearing in another batch for each metric. That means about half of the batches can be implicitly aligned through those interactions (reference compounds), and BatchDTA has the opportunity to model those batches better. (3) We extracted the compound pairs that appeared in multiple batches against the same protein from the datasets and found that the ranking orders of a small number of compound pairs (7.1% to 14.6%) were inconsistent. We suspect the inconsistency is caused by the assay errors, batch identification errors, biological variance, and other factors. Employing BatchDTA to train DNN models can not overcome the impact of those noisy data points. Fortunately, the ranking orders of only less than 1% of all the compound pairs are inconsistent.

We further investigate the impact of the quality of batch identification. Fig. 7 compares the effects of two batch identification methods. For the first method *Batch*, we try our best to distinguish different batches according to the fields recorded in the database. For the second method *Protein*, all the data points with respect to the same protein are grouped in the same batch. Thus, the quality of method *Batch* is higher than that of method *Protein* for batch identification. The results of dataset K_I (Fig. 7(a)) illustrate that the quality of batch identification plays a critical role in the effectiveness of BatchDTA. Besides, for dataset IC_{50}, the CIs of methods *Batch* and *Protein* are comparable. Since IC_{50} is affected by more factors as mentioned, but those factors are not recorded in the database, we can not precisely identify the batches from the database. We believe that the DNN models trained by BatchDTA will benefit from more detailed assay information.

Conclusions

Many advanced studies have applied deep learning to drug-target affinity (DTA) estimation to screen the promising compounds toward the given target proteins. Existing studies focus more on designing DNN model architectures for DTA. We argue that a batch-sensitive training framework, i.e., BatchDTA, can further enhance the accuracy and robustness of the previously proposed DNN models, weakening the influence of batch effects (systematic variance). Each batch is regarded as a ranking task. BatchDTA implicitly aligns the corresponding compounds toward the same protein from multiple batches

bioRxiv preprint doi: https://doi.org/10.1101/2021.11.23.469641; this version posted April 13, 2022. The copyright holder for this preprint (which was not certified by peer review) is the author/funder, who has granted bioRxiv a license to display the preprint in perpetuity. It is made available under aCC-BY-NC-ND 4.0 International license.

Table 2. Statistics of the datasets.

Dataset	Metric	#Compound	#Protein	#Interaction	#Batch
BindingDB	K_D	6,704	587	31,239	1,070
	K_I	126,122	1,225	249,598	11,292
	IC_{50}	407,462	2,582	653,344	20,041
	EC_{50}	75,142	699	105,364	3,143
Davis	K_D	68	442	30,056	442
KIBA	KIBA score	2,111	229	118,254	229

by learning the compounds' ranking orders in each batch. Extensive experimental results demonstrate that four advanced DNN models trained by BatchDTA can achieve significant improvement on three datasets for DTA. BatchDTA can also be applied to train the DNN models on fused data collected from multiple sources to further enhance the models' precision. We believe our work could inspire researchers working on applying machine learning methods to drug discovery.

Appendix: Datasets and Data Process

We describe the details of the data process in this section, and the data statistics of the processed datasets are shown in Table 2.

BindingDB

The BindingDB database with the version of May 2021 contains 2,221,487 compound-protein interactions, including 7,965 proteins and 963,425 compounds.

First, we cleaned up the raw data from BindingDB by the following steps: (1) Keep compound-protein interactions measured by metrics K_D, K_I, IC_{50} and EC_{50}). (2) Remove the recorded affinities with '>' or '<'. (3) Rescale the affinities larger than 10,000 to be 10,000. (4) Drop out the duplicate records. (5) Remove the compounds with illegal SMILES strings that can not be processed by the Cheminformatics software RDKit (https://rdkit.org). (6) Remove the proteins that can not be converted to FASTA format (https://zhanggroup.org/FASTA/).

Second, we identify the batches from the cleaned data: (1) Multiple fields in BindingDB, including 'BindingDB Target Chain Sequence', 'pH', 'Temp (C)', 'Curation/DataSource', 'Article DOI', 'PMID', 'PubChem AID', 'Patent Number', 'Authors', and 'Institution', are considered to identify batches. (2) Remove the batches with less than ten candidate compounds.

Davis and KIBA

We followed the previous work [31] to process Davis and KIBA datasets, and the implementation of which is at `https://github.com/hkmztrk/DeepDTA/tree/master/data`. Then, the batches are identified according to 'Gene ID' for the Davis dataset and 'Uniprot ID' for the KIBA dataset.

Appendix: Relations between Metrics of Binding Affinities

Dissociation constant (K_D), inhibition constant (K_I), half-maximal inhibitory concentration (IC_{50}), and half-maximal effective concentration (EC_{50}) are mainly used for measuring binding affinities. Both K_D and K_I are used to indicate the dissociation equilibrium constant, i.e., the reverse of the association constant, for the dissociated components. K_D is a more general term, while K_I is more specifically used under enzyme-inhibitor complex. IC_{50} is the inhibitory concentration, measured by an inhibitor with the response (or binding) reduced by half. EC_{50} stands for effective concentration of an inhibitor with half-maximal response. Comparing with K_I and K_D, IC_{50} and EC_{50} are influenced by more assay information, such as substrate concentration [17].

In particular, through Cheng-Prusoff equation, K_I can be converted from IC_{50} [19]:

$$K_I = \frac{IC_{50}}{1 + \frac{|S|}{K_m}}, \tag{7}$$

where $|S|$ is the substrate concentration, and K_m is the Michaelis-Menten constant of the substrate. Thus, IC_{50} is assay-specific, and the IC_{50} values under different assay information are incomparable.

In Section. 3.6.1, we evaluate the DNN models that are trained on fused data measured by multiple metrics on the test set of K_I. The data points are added gradually according to the Pearson correlation of the corresponding metrics to K_I. The Pearson correlations are shown in Fig. 8. We first added the data points of K_D, then IC_{50}, and finally EC_{50}.

Appendix: Experimental Settings

Hyper-parameters of BatchDTA

Following the previous works [31, 14, 28, 18], we normalize the original affinities as labels for training. Take K_D for example. We use pK_D values as labels to train the DNN models:

$$pK_D = -log_{10}(\frac{K_D}{10^9}). \tag{8}$$

K_I, IC_{50} and EC_{50} and KIBA score are normalized in the same way.

We used Adam optimizer and applied grid search to explore the best hyper-parameters for each DNN model on each dataset.

For BindingDB database, the candidate settings of each hyper-parameter are shown in Table 3.

For Davis and KIBA datasets, the candidate settings of the hyper-parameters for searching are shown in Table 4.

All the models are trained by NVIDIA Tesla V100 GPUs. Since BatchDTA is a training framework, it would not change the number of model parameters and the time complexity for training.

Generation of Confident Compound Pairs

To generate the confident compound pairs for BindingDB database, we eliminated the compound pairs with small affinity

Draft

bioRxiv preprint doi: https://doi.org/10.1101/2021.11.23.469641; this version posted April 13, 2022. The copyright holder for this preprint (which was not certified by peer review) is the author/funder, who has granted bioRxiv a license to display the preprint in perpetuity. It is made available under aCC-BY-NC-ND 4.0 International license.

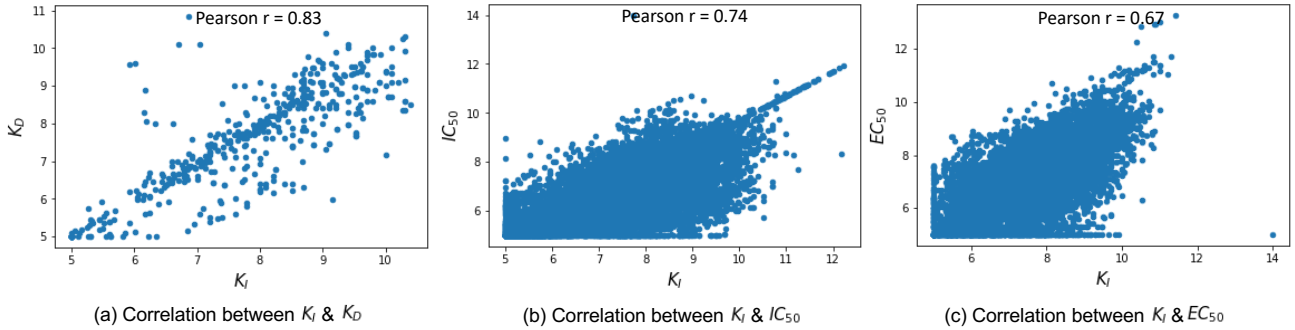

(a) Correlation between K_I & K_D (b) Correlation between K_I & IC_{50} (c) Correlation between K_I & EC_{50}

Fig. 8. Pearson correlations between K_I and other metrics.

Table 3. Candidate settings of hyper-parameters for BindingDB.

Hyper-parameter	Candidate settings
deviation ϵ	{0.2, 0.5, 1}
n_{sample} for K_I	10
n_{sample} for K_D	{1, 3, 5}
n_{sample} for IC_{50}	{0.2, 0.5, 1}
n_{sample} for EC_{50}	{0.1, 0.2, 0.5}
learning rate	$\{1 \times 10^{-3}, 5 \times 10^{-4}\}$
batch size	{256, 512}

Table 4. Candidate settings of hyper-parameters for Davis and KIBA.

Hyper-parameter	Candidate settings
deviation ϵ	{0.2,0.5,1}
n_{sample}	{0.5, 1, 3, 5, 10}
learning rate	$\{1 \times 10^{-3}, 5 \times 10^{-4}\}$
batch size	{256, 512}

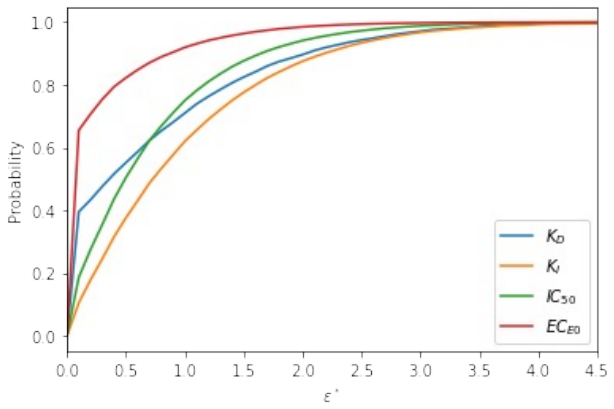

Fig. 9. Probability of the compound pairs with affinity gaps smaller than ϵ^*.

gaps from all the compound pairs. The probability of the compound pairs with affinity gaps smaller than ϵ^* is shown in Fig. 9. When $\epsilon^* = 0.6$, about 50% compound pairs are eliminated.

Appendix: Detailed Results

Overall Performance

Table 5 shows the detailed results corresponding to Fig.3. The DNN models trained by *BatchDTA* framework significantly outperform those trained by *Pointwise* framework in most cases.

Fusing Data Points Measured by Multiple Metrics

Table 6 shows the detailed results corresponding to Fig.5. All the models achieve significant improvement when fusing the data points of K_D. Two models, DeepDTA and GraphDTA(GATGCN), gain significant improvement when fusing the data points of IC_{50}, but no model can get further improvement when fusing the data points of EC_{50}. These results indicate that the data points with higher correlations play a more important role for data argumentation.

Fusing Data Points from Multiple Datasets

Table 7 shows the detailed results corresponding to Fig.6. As we expected, the CIs of the DNN models trained by *BatchDTA* framework significantly surpass those trained by *Pointwise* framework in most cases, consistent with the results in the BindingDB database (refer to Fig. 3). Besides, training on the fusing data points from Davis and KIBA allows the DNN models to achieve better performance than training on a single dataset. Especially when evaluating the models on the KIBA dataset, three models gain significant improvement. Since the KIBA dataset contains only two hundred batches, we suspect that combining four hundred batches from the Davis dataset enhances the richness of batches.

Competing Interests

There is NO Competing Interest.

Code Availability

The code is freely available at GitHub `https://github.com/PaddlePaddle/PaddleHelix/tree/dev/apps/drug_target_interaction/batchdta` to allow replication of the results.

Data Availability

The raw datasets, BindingDB, Davis, and KIBA are collected from `https://www.bindingdb.org/bind/index.jsp`, `http://staff.`

Draft

bioRxiv preprint doi: https://doi.org/10.1101/2021.11.23.469641; this version posted April 13, 2022. The copyright holder for this preprint (which was not certified by peer review) is the author/funder, who has granted bioRxiv a license to display the preprint in perpetuity. It is made available under aCC-BY-NC-ND 4.0 International license.

Table 5. The detailed results corresponding to Fig. 3

Evaluated dataset	K_I			
Evaluated compound pairs	All compound pairs		Confident compound pairs	
Training framework	*Pointwise*	*BatchDTA*	*Pointwise*	*BatchDTA*
DeepDTA	0.6127 (±0.0053)	**0.6252 (±0.0021)**∗	0.6566 (±0.0077)	**0.6775 (±0.0028)**∗
GraphDTA(GCN)	0.6174 (±0.0063)	**0.6347 (±0.0021)**∗	0.6472 (±0.0264)	**0.6929 (±0.0029)**∗
GraphDTA(GATGCN)	0.6168 (±0.0042)	**0.6298 (±0.0036)**∗	0.6600 (±0.0307)	**0.6857 (±0.0053)**
MolTrans	0.6185 (±0.0019)	**0.6559 (±0.0026)**∗	0.6672 (±0.0039)	**0.7204 (±0.0047)**∗

Evaluated dataset	IC_{50}			
Evaluated compound pairs	All compound pairs		Confident compound pairs	
Training framework	*Pointwise*	*BatchDTA*	*Pointwise*	*BatchDTA*
DeepDTA	0.5608 (±0.0042)	**0.5748 (±0.0009)**∗	0.5868 (±0.0081)	**0.5945 (±0.0038)**
GraphDTA(GCN)	0.5527 (±0.0164)	**0.5787 (±0.0002)**∗	0.5606 (±0.0281)	**0.6149 (±0.0004)**∗
GraphDTA(GATGCN)	0.5440 (±0.0090)	**0.5749 (±0.0016)**∗	0.5436 (±0.0379)	**0.6116 (±0.0020)**∗
MolTrans	0.5623 (±0.0037)	**0.5995 (±0.0043)**∗	0.5902 (±0.0071)	**0.6344 (±0.0049)**∗

Note: The standard deviations (std) are given in parenthesis. ∗ stands for the corresponding value is significantly higher than the value on its left (p-value p<0.05) under the T-test with the two-tailed distribution.

Table 6. The detailed results corresponding to Fig. 5

Training framework	BatchDTA			
Training dataset	K_I	K_I&K_D	K_I&K_D&IC_{50}	K_I&K_D&IC_{50}&EC_{50}
DeepDTA	0.6252 (±0.0021)	0.6317 (±0.0021)∗	**0.6368 (±0.0005)**∗	0.6350 (±0.0003)
GraphDTA(GCN)	0.6347 (±0.0021)	**0.6507 (±0.0003)**∗	0.6483 (±0.0019)	0.6488 (±0.0002)
GraphDTA(GATGCN)	0.6298 (±0.0036)	0.6346 (±0.0010)∗	**0.6377 (±0.0065)**∗	0.6363 (±0.0006)
MolTrans	0.6559 (±0.0026)	**0.6595 (±0.0004)**∗	0.6558 (±0.0016)	0.6550 (±0.0015)

Note: The standard deviations (std) are given in parenthesis. ∗ stands for the corresponding value is significantly higher than the value on its left (p-value p<0.05) under the T-test with the two-tailed distribution.

Table 7. The detailed results corresponding to Fig. 6

Evaluated dataset	Davis		
Training framework	Pointwise	BatchDTA	
Training dataset	Davis	Davis	Davis+KIBA
DeepDTA	0.7966 (±0.0074)	0.8028 (±0.0111)	**0.8058 (±0.0085)**
GraphDTA(GCN)	0.7906 (±0.0057)	0.7995 (±0.0044)∗	**0.8046 (±0.0013)**
GraphDTA(GATGCN)	0.7917 (±0.0034)	0.8023 (±0.0009)∗	**0.8038 (±0.0042)**
MolTrans	0.8047 (±0.0083)	0.8079 (±0.0037)	**0.8082 (±0.0054)**

Evaluated dataset	KIBA		
Training framework	Pointwise	BatchDTA	
Training dataset	KIBA	KIBA	KIBA+Davis
DeepDTA	0.7317 (±0.0130)	0.7516 (±0.0138)∗	**0.7631 (±0.0051)**∗
GraphDTA(GCN)	0.7210 (±0.0343)	0.7519 (±0.0052)∗	**0.7568 (±0.0042)**∗
GraphDTA(GATGCN)	0.7140 (±0.0210)	0.7520 (±0.0059)∗	**0.7561 (±0.0013)**
MolTrans	0.7392 (±0.0066)	0.7588 (±0.0115)∗	**0.7733 (±0.0060)**∗

Note: The standard deviations (std) are given in parenthesis. ∗ stands for the corresponding value is significantly higher than the value on its left (p-value p <0.05) under the T-test with the two-tailed distribution.

`cs.utu.fi/~aatapa/data/DrugTarget/` and `https://jcheminf.biomedcentral.com/articles/10.1186/s13321-017-0209-z`. The processed data is available at GitHub `https://github.com/PaddlePaddle/PaddleHelix/tree/dev/apps/drug_target_interaction/batchdta` to allow replication of the results.

Author Contributions Statement

XM.F., F.W., H.W., and HF.W. led the research. HY.L, YF.X, XM.F., and F.W. conceived the experiments. HY.L. YF.X, and W.L.conducted the experiments. LY.L, XM.F., and YF.X. wrote the manuscript.

Draft

bioRxiv preprint doi: https://doi.org/10.1101/2021.11.23.469641; this version posted April 13, 2022. The copyright holder for this preprint (which was not certified by peer review) is the author/funder, who has granted bioRxiv a license to display the preprint in perpetuity. It is made available under aCC-BY-NC-ND 4.0 International license.

Acknowledgments

The authors thank the anonymous reviewers for their valuable suggestions.

References

1. Joshua M Akey, Shameek Biswas, Jeffrey T Leek, and John D Storey. On the design and analysis of gene expression studies in human populations. *Nature genetics*, 39(7):807–808, 2007.
2. Sylvain Arlot and Alain Celisse. A survey of cross-validation procedures for model selection. *Statistics surveys*, 4:40–79, 2010.
3. Keith A Baggerly, Sarah R Edmonson, Jeffrey S Morris, and Kevin R Coombes. High-resolution serum proteomic patterns for ovarian cancer detection. *Endocrine-related cancer*, 11(4):583–584, 2004.
4. Chris Burges, Tal Shaked, Erin Renshaw, Ari Lazier, Matt Deeds, Nicole Hamilton, and Greg Hullender. Learning to rank using gradient descent. In *Proceedings of the 22nd international conference on Machine learning*, pages 89–96, 2005.
5. Ruolan Chen, Xiangrong Liu, Shuting Jin, Jiawei Lin, and Juan Liu. Machine learning for drug-target interaction prediction. *Molecules*, 23(9), 2018.
6. Anna Cichonska, Tapio Pahikkala, Sandor Szedmak, Heli Julkunen, Antti Airola, Markus Heinonen, Tero Aittokallio, and Juho Rousu. Learning with multiple pairwise kernels for drug bioactivity prediction. *Bioinformatics*, 34(13):i509–i518, 2018.
7. Anna Cichonska, Balaguru Ravikumar, Elina Parri, Sanna Timonen, Tapio Pahikkala, Antti Airola, Krister Wennerberg, Juho Rousu, and Tero Aittokallio. Computational-experimental approach to drug-target interaction mapping: a case study on kinase inhibitors. *PLoS computational biology*, 13(8):e1005678, 2017.
8. Jelena Čuklina, Patrick GA Pedrioli, and Ruedi Aebersold. Review of batch effects prevention, diagnostics, and correction approaches. In *Mass spectrometry data analysis in proteomics*, pages 373–387. Springer, 2020.
9. Mindy I Davis, Jeremy P Hunt, Sanna Herrgard, Pietro Ciceri, Lisa M Wodicka, Gabriel Pallares, Michael Hocker, Daniel K Treiber, and Patrick P Zarrinkar. Comprehensive analysis of kinase inhibitor selectivity. *Nature biotechnology*, 29(11):1046–1051, 2011.
10. Joseph L. Durant, Burton A. Leland, Douglas R. Henry, and James G. Nourse. Reoptimization of MDL keys for use in drug discovery. *J. Chem. Inf. Comput. Sci.*, 42(5):1273–1280, 2002.
11. Mithat Gönen and Glenn Heller. Concordance probability and discriminatory power in proportional hazards regression. *Biometrika*, 92(4):965–970, 2005.
12. Laleh Haghverdi, Aaron T L Lun, Michael D Morgan, and John C Marioni. Batch effects in single-cell rna-sequencing data are corrected by matching mutual nearest neighbors. *Nature Biotechnology*, 36(5):421–427, 2018.
13. Jun Han and Claudio Moraga. The influence of the sigmoid function parameters on the speed of backpropagation learning. In *International workshop on artificial neural networks*, pages 195–201. Springer, 1995.
14. Tong He, Marten Heidemeyer, Fuqiang Ban, Artem Cherkasov, and Martin Ester. Simboost: a read-across approach for predicting drug–target binding affinities using gradient boosting machines. *Journal of cheminformatics*, 9(1):1–14, 2017.
15. Sepp Hochreiter and Jürgen Schmidhuber. Long short-term memory. *Neural computation*, 9(8):1735–1780, 1997.
16. Kexin Huang, Cao Xiao, Lucas M Glass, and Jimeng Sun. Moltrans: Molecular interaction transformer for drug–target interaction prediction. *Bioinformatics*, 37(6):830–836, 2021.
17. Edward C Hulme and Mike A Trevethick. Ligand binding assays at equilibrium: validation and interpretation. *British journal of pharmacology*, 161(6):1219–1237, 2010.
18. Mingjian Jiang, Zhen Li, Shugang Zhang, Shuang Wang, Xiaofeng Wang, Qing Yuan, and Zhiqiang Wei. Drug–target affinity prediction using graph neural network and contact maps. *RSC Advances*, 10(35):20701–20712, 2020.
19. Tuomo Kalliokoski, Christian Kramer, Anna Vulpetti, and Peter Gedeck. Comparability of mixed ic50 data–a statistical analysis. *PloS one*, 8(4):e61007, 2013.
20. Alex Krizhevsky, Ilya Sutskever, and Geoffrey E Hinton. Imagenet classification with deep convolutional neural networks. *Advances in neural information processing systems*, 25:1097–1105, 2012.
21. Yann LeCun, Yoshua Bengio, et al. Convolutional networks for images, speech, and time series. *The handbook of brain theory and neural networks*, 3361(10):1995, 1995.
22. Ingoo Lee, Jongsoo Keum, and Hojung Nam. Deepconv-dti: Prediction of drug-target interactions via deep learning with convolution on protein sequences. *PLoS computational biology*, 15(6):e1007129, 2019.
23. Jeffrey T Leek, W Evan Johnson, Hilary S Parker, Andrew E Jaffe, and John D Storey. The sva package for removing batch effects and other unwanted variation in high-throughput experiments. *Bioinformatics*, 28(6):882–883, 2012.
24. Jeffrey T Leek, Robert B Scharpf, Héctor Corrada Bravo, David Simcha, Benjamin Langmead, W Evan Johnson, Donald Geman, Keith Baggerly, and Rafael A Irizarry. Tackling the widespread and critical impact of batch effects in high-throughput data. *Nature Reviews Genetics*, 11(10):733–739, 2010.
25. Tiqing Liu, Yuhmei Lin, Xin Wen, Robert N Jorissen, and Michael K Gilson. Bindingdb: a web-accessible database of experimentally determined protein–ligand binding affinities. *Nucleic acids research*, 35(suppl_1):D198–D201, 2007.
26. Yunan Luo, Xinbin Zhao, Jingtian Zhou, Jinglin Yang, Yanqing Zhang, Wenhua Kuang, Jian Peng, Ligong Chen, and Jianyang Zeng. A network integration approach for drug-target interaction prediction and computational drug repositioning from heterogeneous information. *Nature Communications*, 8(1):573, 2017.
27. Ricardo Macarron, Martyn N. Banks, Dejan Bojanic, David J. Burns, Dragan A. Cirovic, Tina Garyantes, Darren V. S. Green, Robert P. Hertzberg, William P. Janzen, Jeff W. Paslay, Ulrich Schopfer, and G. Sitta Sittampalam. Impact of high-throughput screening in biomedical research. *Nature Reviews Drug Discovery*, 10(3):188–195, 2011.
28. Thin Nguyen, Hang Le, Thomas P Quinn, Tri Nguyen, Thuc Duy Le, and Svetha Venkatesh. GraphDTA: predicting drug–target binding affinity with graph neural networks. *Bioinformatics*, 37(8):1140–1147, 10 2020.
29. Tri Minh Nguyen, Thin Nguyen, Thao Minh Le, and Truyen Tran. Gefa: early fusion approach in drug-target affinity

Not Certified

bioRxiv preprint doi: https://doi.org/10.1101/2021.11.23.469641; this version posted April 13, 2022. The copyright holder for this preprint (which was not certified by peer review) is the author/funder, who has granted bioRxiv a license to display the preprint in perpetuity. It is made available under aCC-BY-NC-ND 4.0 International license.

prediction. *IEEE/ACM Transactions on Computational Biology and Bioinformatics*, 2021.

30. Rıza Özçelik, Hakime Öztürk, Arzucan Özgür, and Elif Ozkirimli. Chemboost: A chemical language based approach for protein–ligand binding affinity prediction. *Molecular Informatics*, 2020.
31. Hakime Öztürk, Arzucan Özgür, and Elif Ozkirimli. DeepDTA: deep drug–target binding affinity prediction. *Bioinformatics*, 34(17):i821–i829, 09 2018.
32. Hakime Öztürk, Elif Ozkirimli, and Arzucan Özgür. Widedta: prediction of drug-target binding affinity. *arXiv preprint arXiv:1902.04166*, 2019.
33. David Rogers and Mathew Hahn. Extended-connectivity fingerprints. *J. Chem. Inf. Model.*, 50(5):742–754, 2010.
34. Bonggun Shin, Sungsoo Park, Keunsoo Kang, and Joyce C Ho. Self-attention based molecule representation for predicting drug-target interaction. In *Machine Learning for Healthcare Conference*, pages 230–248. PMLR, 2019.
35. Marta M Stepniewska-Dziubinska, Piotr Zielenkiewicz, and Pawel Siedlecki. Development and evaluation of a deep learning model for protein–ligand binding affinity prediction. *Bioinformatics*, 34(21):3666–3674, 2018.
36. Jing Tang, Agnieszka Szwajda, Sushil Shakyawar, Tao Xu, Petteri Hintsanen, Krister Wennerberg, and Tero Aittokallio. Making sense of large-scale kinase inhibitor bioactivity data sets: a comparative and integrative analysis. *Journal of Chemical Information and Modeling*, 54(3):735–743, 2014.
37. Ashish Vaswani, Noam Shazeer, Niki Parmar, Jakob Uszkoreit, Llion Jones, Aidan N Gomez, Ł ukasz Kaiser, and Illia Polosukhin. Attention is all you need. In I. Guyon, U. V. Luxburg, S. Bengio, H. Wallach, R. Fergus, S. Vishwanathan, and R. Garnett, editors, *Advances in Neural Information Processing Systems*, volume 30. Curran Associates, Inc., 2017.
38. Wei Zhou, Karel K. M. Koudijs, and Stefan Böhringer. Influence of batch effect correction methods on drug induced differential gene expression profiles. *BMC Bioinformatics*, 20(1):437, 2019.

Draft